

---

# Simulation of Anti Reflecting Coating for Improving External Quantum Efficiency of Photovoltaic Cell

---

Jai Prakash<sup>1\*</sup>, Kalpana Meena<sup>2</sup>

<sup>1\*</sup>PG Scholar, Department of EE, Rajasthan Institute of Engineering and Technology, Jaipur

<sup>2</sup>Assistant Professor, Department of EE, Rajasthan Institute of Engineering and Technology, Jaipur

Email: <sup>2</sup>ee.kalpana@rietjaipur.ac.in

Corresponding Email: <sup>1\*</sup>jpsolanki1995@gmail.com

Received: 08 April 2022

Accepted: 25 June 2022

Published: 28 July 2022

**Abstract:** *Due to a dramatic drop in solar module prices/watt peaks, photovoltaic (PV) electricity has become more concentrated over the last decade. Crystallized silicon (c-Si) solar cells have dominated the solar market since their creation, outperforming all other photovoltaic technologies. PV modules are frequently required to work in inclement weather. Outdoor photovoltaic performance is affected by a number of factors, including*

*1) Solar radiation, 2) the shape of the absorbed solar spectrum, 3) ambient temperature, 4) location, 5) wind speed, and 6) aerosols. These parameters, on the other hand, are out of our hands. It does not prevent solar panels from becoming heated on hot days, which has a negative impact on their electrical performance and longevity. To protect the solar cell from various external variables, multiple layers are applied to solar cell modules, including EVA (Ethylene Vinyl Acetate), polyvinyl fluoride sheet (Tedlar), front solar glass, metal frame, and side water seal. One of the main causes of the absorber layer temperature in solar modules rising is this. For single-layer and multi-layer ARC designs, a range of materials are used in the ARC of solar modules. Instead of functioning as a radiative cooler, the ARC can be changed or simple tweaks can be made to improve absorption and lower the temperature of the solar module. Based on light and radiation properties, choose materials for SR-ARC design of solar cells and modules. The chosen material must have very low absorption between 300 and 1200 nm and emit between 8 and 13  $\mu$ m. The annual power generation of a 1kW system in India's complicated environment is determined with the aforesaid efficiency increases and temperature reductions. From a single layer c-Si solar module system, the double layer module of the 1kW system generates 54kWh. Furthermore, the cooling effect was calculated, with the failed component losing 80% of its initial efficiency by the end of 2014, but the two- and three-layer components reached this level by the end of 36. The dual layer SR-ARC coated module system will start producing single layer modules at the end of 26 or 36, with or without replacement.*

**Keywords:** *Photovoltaic (PV), Crystallized Silicon (C-Si), Solar Cells, EVA (Ethylene Vinyl Acetate), Polyvinyl Fluoride Sheet.*

## 1. INTRODUCTION

Governments will help relieve the burden by reducing the use of grid power systems or grids and re-conserving electricity as more people turn to green energy sources such as solar, wind, and geothermal, which are available to consumers of the Electricity Commission or the government.

Solar energy is converted directly into electricity using photovoltaic power generating. It generates power using sunlight and produces no pollutants or greenhouse gases. The solar cell effect was discovered in 1839 by French physicist Edmund Becquerel. Einstein also wrote a paper on photovoltaics and photocarrier energy in 1905, which sparked renewed interest in solar energy and its possibilities. The first practical silicon solar cell was demonstrated in 1954 by Bell Labs [1]. In the initial stage, the efficiency of the solar cell was about 4%, since then there is a huge improvement in solar cell efficiency and technology. Single-junction and multi-junction solar cells have recently been found to have maximum efficiency of roughly 26.7% and 38.8%, respectively [2] and [3]. Single-junction and multi-junction solar cells, on the other hand, can still be improved. Single-contact solar cells, on the other hand, can achieve 33.7% efficiencies [4].

Crystalline Silicon (c-Si) PV technology having more than 90% market share of today's world PV technologies. It is mainly because the technology is having direct benefits from the electronics industry. This technology directly adopted many processes which are already used by the electronics industry to develop pure silicon. This technology uses a non-toxic and abundant amount of materials available on the earth. The global PV market has grown exponential in the last 15 years. In 2018 about 103 GW has been installed and the same trend has been seen the last year 2019. The total installed capacity at the end of 2018 is about 512.3GW [5].

On the 11th January 2010, the national solar mission launched in India targeting 20000 MW, however, in 2015 the government revised and boosted the target of the grid-connected solar PV project to 100,000 MW by the year of 2021-22 [6]. As per Ministry of power, India, in 2018-19, the overall growth rate of energy generation is 5.19%, in which the generation growth rate of renewable energy is about 24.47% in 2018-19. As on 30th September 2019 installed capacity of power generator is about 363,370MW in which thermal power plant capacity is about 63.2% whereas the renewable energy contribution is about 22.7% in total installed capacity [7].

The efficiency drops by 0.45% for every 1°C increase in temperature, while the degradation rate of the components doubles for every 10°C increase in temperature [8]. As a result, it's critical to keep the solar module's temperature down. Due to degradation losses of high-energy photons, parasitic losses of low-energy photons, and resistive losses, the PV temperature is 20°C to 30°C higher than the ambient temperature as mentioned in the preceding paragraph. In Indian summer this temperature goes up to 75 °C. This reduces the durability and performance of the solar module. The generated heat tries to evacuate from the solar module through top and bottom surface, but due to low conductive heat transfer coefficient of EVA and Tedlar it does not evacuate quickly, and that raises the temperature of the module. Active and passive cooling



technologies have been used to cool solar cells and modules.

### **Literature Survey:**

Solar energy is a never-ending source of energy. Everything which we are getting from nature is solar energy either in the direct or indirect form. From the initial time of human civilization, it was harnessed in the different form of energy. Solar energy received by the earth surface is in the form of solar irradiance. It is the small portion of electromagnetic radiation emitted by the Sun, which mainly contains infrared, visible and ultraviolet spectra. However, the received irradiance is varying from the location (latitude and longitude) and the height of the location (altitude). It is mainly due to atmospheric condition and time of the day. The direct normal and the global normal, according to the American Society for Testing and Materials (ASTM), are two sections of the Earth's solar spectrum (the hemispheres in the two stellar field of view of the measurement plane). The direct normal spectrum is included in ASTM G-173-03 [9], which also includes the global global spectrum. AM1.5G is the standard solar irradiance received by the Earth's surface, where AM refers for near-end and G stands for Earth's spectrum. The base end is the smallest possible path length that normalises the light. The solar cell is the fundamental component of a solar photovoltaic module, with the primary function of absorbing solar energy and producing an electron-hole pair. For the movement of electron-hole pair from the absorber layer to external circuit mainly because of the depletion region which forms mainly because of the p and n-type doped material has been fused. The minority charge carrier separated at the p-n junction and collected by the external circuit. The energy of incident photons is higher than the band gap that can generate electron-hole pairs. However, heat is converted from more excess energy (direct and indirect) than the band gap. Other recombination and low-energy photons absorbed by the solar cell and other extra layers, on the other hand, generate heat and raise the solar cell's temperature [10].

To get a certain voltage and current from the output, solar cells can be linked in series and/or parallel. Based on peak power and efficiency the solar cells are grouped in a different section. To minimize the mismatch losses in solar module cell are connected on the basis of their similar or equal properties. The solar cell is very fragile from mechanical forces and environmental factors like a thermal cycle, dust and rain etc. Thus, for the protection of solar cells in long term operation, they are encapsulated by the different component like front glass, EVA, Encapsulated solar cell string, and back sheets. The solar module has been tested at a lab (indoor environment) for the standardization at standard testing condition (STC, 1000 Wm<sup>-2</sup>, 25 °C, AM1.5 solar spectrum and wind speed is 1 ms<sup>-1</sup>) [11]. However, in outdoor conditions, the performance of the solar module is influenced by a number of uncontrollable factors like as solar irradiance and angle of incidence, ambient and module temperature, wind speed, installation site, and aerosol [12] [19]. The outdoor condition of the environment is changing every time of the day, month and throughout the year. As we all know, environmental factors have a positive and negative impact on the solar cell's/numerous modules output parameters. Whereas the module tested for 25 °C but the ambient temperature came in the range of 30 °C-45 °C in composite climate, place like Jaipur. Due to low conversion, recombination and parasitic absorption, the temperature of the module goes up to 60 °C -75 °C [17], [20] [27]. The output of solar cells is known to be influenced by temperature [28]. The current temperature coefficient, on the other hand, has a positive value that is very low in relation to the temperature, and the voltage

temperature coefficient has a negative value that is larger than the current temperature coefficient [29-30]. Due to that, the efficiency of solar PV starts to reduce with the increment of temperature. A different study shows that each deg rise in temperature efficiency of the PV module reduces by 0.45% [20]. Along with the efficiency drop, the temperature rise also affects the life of the PV module. Each 10 °C rise in temperature ageing of the module will bedouble [8]. Dupré et al. have designed a thermal model of photovoltaic to describe the physics of absorption, conversion and losses of the photovoltaic module [31].

The number of electron-hole pairs gathered to the number of photons received is referred to as quantum efficiency (QE). When photons of a specific wavelength are impinge on the solar cell, the quantum efficiency value represents the amount of current the cell produces. When this value is multiplied by the solar spectrum, the solar cell generates a total current when exposed to light. Quantum efficiencies are divided into two categories.

- The ratio of charge carriers gathered by a solar cell to the number of photons (incident photons) dropping out of the solar cell is called external quantum efficiency (EQE).
- The ratio of charge carriers collected by a solar cell to photons absorbed by the solar cell is known as internal quantum efficiency (IQE).

The EQE depends on both absorption of photons as well as the collection of photons whereas the IQE is the material properties of the solar cell. Light is the electromagnetic wave which shows the wave-like properties as well as the particle nature also. When the light is treated as the particle then it called Photons [83]. The energy of every single photon is proportional to the frequency of the photon's propagation. The total energy is the integral of the photons number in a particular wavelength. The quantum theory of light describes the relationship between the frequency and energy of light. Planck has established the relation between these two quantities through a constant. Where the speed of light is also a constant and only variable is the frequency of the photons. Based on this relation, the energy of the photons has been calculated in terms of eV. The Planck's constant and speed of light multiplication is about 1240eV nm. The crystalline silicon solar cells having a bandgap of 1.1eV. The number of absorbed photons of the solar spectrum in a c-Si solar cell having more energy than the bandgap can generate electron-hole pair. Figure 1 the solar spectrum and the number of photons in a particular wavelength has been mentioned.

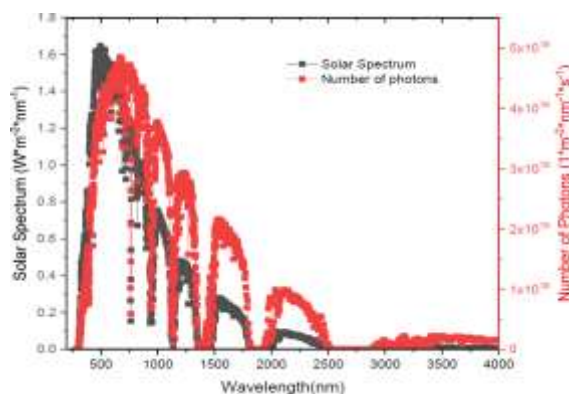


Figure 1: The solar spectrum and the number of photons in a particular wavelength [84]

Any materials contain some heat emit the electromagnetic waves and it is called electromagnetic radiation. Radiation is emitted by all matter in the universe that is not pure spirit. The frequency of radiation, however, is determined by the dark body's temperature. All incoming radiation is absorbed, not reflected, by blackbody materials. A black body absorbs the same amount of radiation as it emits at a given temperature, according to Gustav Kirchhoff. Planck's back-body radiation law, Wien's displacement law, Stefan-Boltzmann law, and Limber's cosine law [85] are only a few examples of correlations between emission spectrum and temperature.

Various technologies have been tested for their energy yield due to variation in the solar spectrum. They have studied for four different locations for eight different technologies during one year and found that the higher bandgap technology monthly spectral gain is noticeable [86]. For the CdTe PV technology, the spectral response has been investigated for the different season in the composite climate of India [14].

### **Contribution of the Present Work**

The main purpose of this research is to lower the operating temperature of solar modules in order to improve their performance and lifetime outside. The contributions to the present task are summarised in the table below.

1. To understand operational concerns and the most fission-prone solutions, the literature on solar cell/module temperature rise will be thoroughly searched. Further, the new methodology has been developed to optimize the solution based on the requirement.
2. Initial work was done to find out the best suitable material for the radiative cooling which can be simultaneously used as an antireflective coating. These material properties have been discussed for the optical and thermal point of view.
3. Furthermore, multilayer ARCs are used to discuss the feasibility of radiative cooling of solar cells. A boost in efficiency was discovered on this basis.
4. A new form of anti-reflection coating is being developed for commercial solar cells, with the potential to reduce the operating temperature of solar modules by more than 5°C.
5. The lifespan and power generation of the solar cells/modules are evaluated based on the temperature drop when compared to conventional solar cells/modules.

### **Problem Statement:**

The lifetime of a solar photovoltaic module is the duration of time after which module cannot be used because of cost of production, land cost, safety issues and the output power has been reduced below the acceptable values[213]. The module manufacturer gives guarantee for the module power output above the certain values for the certain period like for crystalline silicon solar module efficiency must be above the 80% for 25 years. The experimental result shows that the module degradation is behaving almost linear but in actual it is an exponential decay. However due to the short period of time the pattern of exponential decay not able to clear. This is one of the most important factors which have direct impact on the cost of power production. In the PV module degradation rate has been taken very aggressively about 0.5%, whereas the PV systems average degradation is about 0.8% and many systems are worse in reality [204].

## 2. PROPOSED METHOD

The external quantum efficiency (EQE), reflection and transmittance, current-voltage curve (I-V curve), and sample texture height were all calculated using five 0.157\*0.157m<sup>2</sup> c-Si solar samples. Every 5 samples, all of these variables were assessed.

For solar cell internal quantum efficiency (IQE) calculations, estimate the reflectance (R) and transmittance (T) in the range of 280 nm to 2500 nm. The transmittance of a c-Si solar cell is 0 in a certain range because the backside is coated with silver (Ag). Measure the EQE between 300nm and 1100nm for c-Si solar cell samples.

$$IEQ = \frac{EQE}{1-\rho}$$

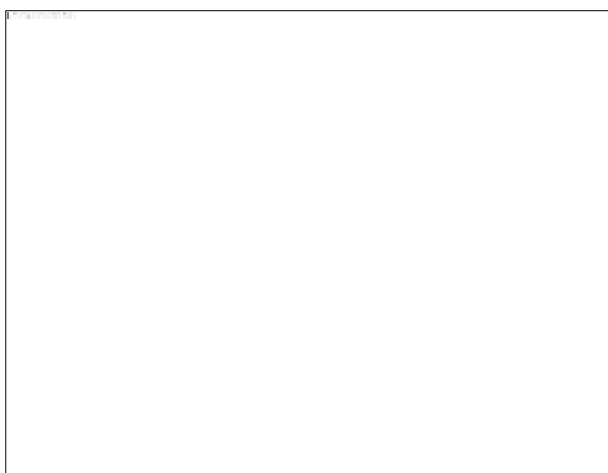


Fig 2: Reflectivity of the c-Si solar cell

On The IQE and current density ( $J_{sc}$ ) have been computed using the measured EQE, reflection, transmittance, and solar spectrum [214].

$$J_{sc} = -q \int_{\lambda_1}^{\lambda_2} EQE(\lambda) * \Phi_{ph,\lambda}^{AM1.5} * d\lambda$$

Where  $q$  is the charge of the electron ( $1.60217662 \times 10^{-19}$  coulombs),  $\phi$  is the spectral photons flux at AM1.5 in the range of 300-1100 nm wavelength ( $\lambda$ ) range.

From the measured EQE and absorbed photon flux, the single-layer ARC c-Si solar cell current density is around 34.28mA cm<sup>-2</sup>. STC (Standard Testing Condition) measures the solar cell's I-V curve, which is depicted in Figure 3.2 with various parameters. Voltage, current, series, and shunt resistance are all represented by the I-V characteristics of solar cells, and these parameters are used to compute solar cell efficiency and charge rate.

Solar cells operate at a higher temperature outside than they do inside, and the parameters are also affected by the operating temperature. When SR-ARC is used, the operating temperature will change.

IEC60891 2nd Edition [215], [216] were used to estimate various parameters for SR-ARC

polycrystalline silicon (mc-Si) solar modules and individual ARC-mc-Si solar modules. The efficiency of photovoltaic modules is expected to rise with the operating temperature and solar cell absorption rate, based on the factors listed above. According to IEC60891 procedure 1, the I-V curve from the STC to the operating temperature module was transformed.

$$I_r = I_m + I_{sc} \left( \frac{G_r}{G_m} - 1 \right) + \alpha_i (T_r - T_m)$$

$$V_r = V_m - R_s (I_r - I_m) - \kappa I_r (T_r - T_m) + \beta (T_r - T_m)$$

Here  $\alpha_i$  is the temperature coefficients of short circuit current,  $\kappa$  is the curve correction factor,  $\beta$  is the temperature coefficients of open-circuit voltage.  $R_s$  is the series resistance of the solar module.  $I_r$  is the rated current at rated temperature ( $T_r$ ) and rated radiation ( $G_r$ ) with respect to measured temperature ( $T_m$ ) and radiation ( $G_m$ ) from measured current ( $I_m$ ) and the short circuit current ( $I_{sc}$ ), further the rated voltage has been calculated with the help of measured voltage ( $V_m$ ).

The above equation also gives a clear idea of the effect of solar radiation. It is well known that solar radiation varies with the change in weather condition and the time of the day.

Deterioration of solar cells/modules has been extensively investigated in the literature, with thermal cycling and high temperatures being linked to all types of degradation [16], [185], [186]. For every 10°C rise in temperature, the ageing rate of solar cells doubles [8, 58]. Manufacturers use degradation rates of 0.6 percent to 0.5 percent per year in their PV cost calculations, but degradation rates in climatic settings like India are 1.4 percent to 0.7 percent per year [12], [188]. The module's life is also impacted by the deterioration indicated above. One of the most important elements influencing the cost of photovoltaic is module longevity, which is well known. It can be calculated using the Arrhenius equation at a given temperature. The ageing rate of single, double, and triple layer ARC has been calculated at different temperatures of the solar module.

$$\text{Rate of Ageing} = e^{\left(\frac{-E_a}{kT}\right)}$$

Here,  $E_a$  is the effective activation energy, which is 0.6 eV [222],  $k$  is the Boltzmann constant (in electric volts), and  $T$  is the solar module's temperature in Kelvin.

As seen below, the rate of degradation changes as the temperature of the solar module changes.

$$d = \frac{\text{Rate of Aging at } T_{new}}{\text{Rate of Aging at } T_{base}} * D$$

$D$  is the degradation rate of the solar module with the single layer ARC at room temperature, and  $d$  is the change in degradation rate as a function of temperature. The single-layer mc-Si solar module's base temperature is  $T_{base}$ . The temperature of the SR-ARC coated module's double or triple layers is  $T_{new}$ .

$$C = C^0 e^{-d*t}$$

Here,  $t$  is the length of time (in years),  $C$  denotes the capacity after  $t$  years, and  $C^0$  denotes the



original capacity. The initial module generating capacity is estimated to be 100 percent, with a first-year decline of roughly 2.5 percent. It is also assumed that the module will degrade at a rate of 0.8 percent per year with SR-ARC and 0.5 percent per year without it.

Throughout the project, numerous assumptions were formed. A number of factors influence the transmittance of an empty atmosphere window. All computations, however, were completed in the presence of a clear sky. It was not possible to compute emissivity in cloudy conditions.

The simulation model adopts the average surface height and base of the unit pyramid, despite the fact that the surface of the solar cell is not uniform across the stack. The top and bottom of the solar cell/module are defined limits, while the four sides are essentially periodic and repeat in all directions. To decrease reflections from top and bottom surfaces, imagine layers that are perfectly matched. The side edges of the solar modules are insulated during the simulation of heat transmission. The deterioration of the components is dependent on several elements, as detailed in the literature, in the life calculation procedure.

### 3. RESULTS AND DISCUSSION

The material properties and other factors utilised in the mathematical simulation are listed in Table 1. It also depicts the thermal conductivity differences between c-Si-EVA and EVA-low iron solar glass. Low-iron solar glass has a transmittance ranging from 4 to 25 metres. After putting the laminate (EVA and front glass) to the solar cell, the actual output of the SR-ARC was estimated over the wavelength range of 4µm to 25µm. In the wavelength range of 4µm to 25µm [198], EVA also has high transmittance.

Table 1: The various material properties and other parameters for the mathematical simulation

Input Parameters	Details
Geometry	Nanoparticle size range: 5–50 µm
Nanoparticles Composite antireflection coatings Materials-material	SiO <sub>2</sub> , Si <sub>3</sub> N <sub>4</sub> , Al <sub>2</sub> O <sub>3</sub> , TiO <sub>2</sub> , and ZnO used as Composite material antireflection coatings
Model Physics	<ul style="list-style-type: none"> <li>• Top and bottom surfaces: Periodic</li> </ul>
Mesh size	Physics-controlled mesh with element size (Fine)
Study	<ul style="list-style-type: none"> <li>• Type: Wavelength domain                             <ul style="list-style-type: none"> <li>• Unit: λ (µm)</li> </ul> </li> <li>• Range: 0.380–0.720 µm, with resolution: 10 µm</li> </ul>

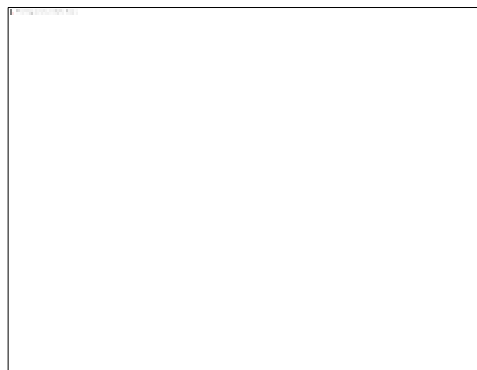


Fig 3: Reflectivity Bar chart

From the measured EQE and absorbed photon flux, the single-layer ARC c-Si solar cell current density is around  $34.28\text{mA cm}^{-2}$ . STC (Standard Testing Condition) measures the solar cell's I-V curve, which is depicted in Figure 4 with various parameters. Voltage, current, series, and shunt resistance are all represented by the I-V characteristics of solar cells, and these parameters are used to compute solar cell efficiency and charge rate.

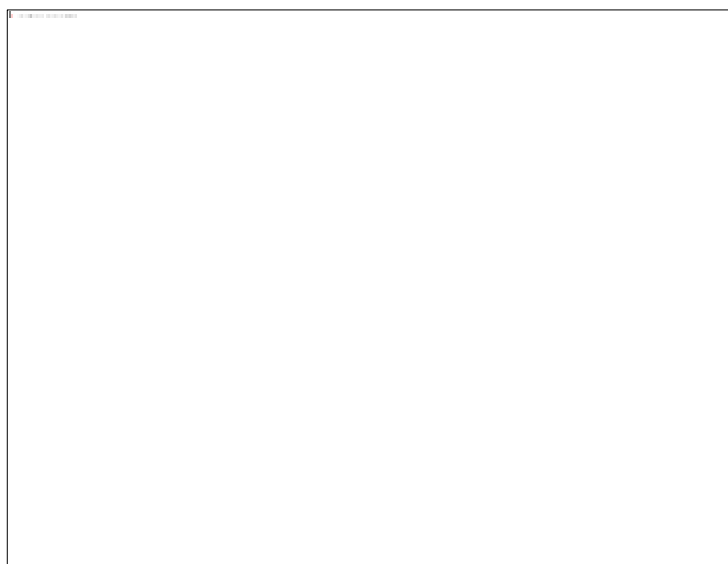


Figure 4: I-V curve of the solar cell

Wind speed, base, altitude, latitude, longitude, humidity, pollution, and visibility are all taken into account while generating the solar spectrum. The solar spectrum was altered as the bottom edge shifted from 1 to 4.5 and the humidity increased from 10% to 90%. Changes in the sun spectrum and ambient temperature are used to calculate how much power photovoltaic modules generate. In Figure 5, wavelength variations in the sun spectrum are clearly visible.

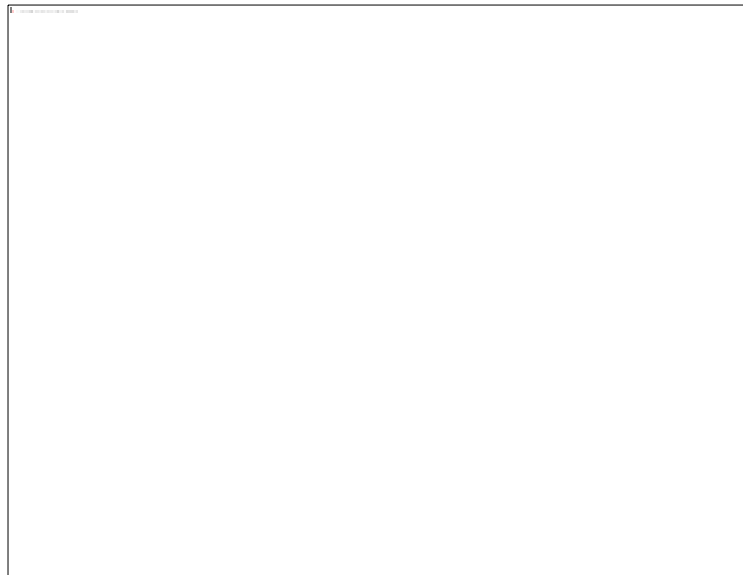


Figure 5: Solar spectrum variation due to Air Mass and Humidity [217]

#### 4. CONCLUSION

The new I-V of the solar module has been determined using absorption in the c-Si solar module and temperature reduction in the double-layer SR-ARC solar module. It was determined based on the Pmax. The comparison between the single layer and double layer SR-ARC modules is shown. The module efficiency has improved by 0.22 percent from singlelayer to double layer at STC, and the fill factor has improved by 0.38 percent, primarily due to temperature adjustment and modest absorption enhancement. Initially, the ambient temperature of 30 °C and both the module absorption in 300 nm- 1200 nm is constant. Firstly, the single-layer operating temperature has been calculated based on emission and electrical generation at an average ambient temperature of 30°C. Further, the double- layer SR-ARC STC has been corrected for its Jsc that was calculated on the absorption of c-Si with the application of double-layer SR-ARC. The basic structure (c-Siwafer) of both single- and double-layer module are similar, due to that the IQE of these modules is the same. Based on IEC 61853 procedure-1, the performance of both modules has been tested in the range of 15 °C -75 °C module temperature and solar radiation is in the range of 100 Wm<sup>-2</sup> to 1100 Wm<sup>-2</sup>. This standard gives more realistic idea about the performance of the solar module in various environmental conditions.

#### 5. REFERENCES

1. D. Ghernaout, A. Alghamdi, M. Touahmia, M. Aichouni, N. A. Messaoudene, "Nanotechnology Phenomena in the Light of the Solar Energy", Journal of Energy, Environmental & Chemical Engineering, vol. 31, 2018, pp: 1-8.
2. D. Davchevski, "How to Increase Human Energy According to Tesla", Uplift, Science, December 2016.
3. K. V. Baryshnikova, V. E. Babicheva, P. A. Belov, M. I. Petrov, "Substratemediated



- antireflective properties of silicon nanoparticle array”, IEEE, Day on Diffraction, International Seminar, December 2016.
4. R. Gore, H. Satheesh, M. Varier, S. Valsan, “Analysis of an IEC 61850 based Electric Substation Communication Architecture”, IEEE, 7th International Conference on Intelligent Systems, Modelling and Simulation (ISMS), Bangkok, Thailand, January 2016.
  5. D. Michaelson, H. Mahmood, J. Jiang, “A Predictive Energy Management System Using Pre-Emptive Load Shedding for Islanded Photovoltaic Microgrids”, IEEE Transactions on Industrial Electronics, Vol. 64, Issue. 7, July 2017, pp:5440 – 5448.
  6. Choi, J.-Y., I. Kim, and G. E. Jabbour, “Enhanced surface passivation of colloidal CdSe nanocrystals for improved efficiency of nanocrystal/polymer hybrid solar cells”, IEEE Journal of Photovoltaics, vol. 6(5), July 2016, pp: 1203–09.
  7. U. Mehmood, I. A. Hussein, A. Al-Ahmed, and S. Ahmed, “Enhancing power conversion efficiency of dye-sensitized solar cell using TiO<sub>2</sub> - MWCNT composite photoanodes”, IEEE J. Photovoltaics, vol. 6, Issue 2, March 2016, pp: 486–490.
  8. Y. LePing, D. Tune, C. Shearer, T. Grace, J. Shapter, “Heterojunction solar cells based on silicon and composite films of polyaniline and carbon nanotubes”, IEEE Journal of Photovoltaics, vol. 6 (3), pp: 688–95.
  9. Rebekah L. Garris ; Lorelle M. Mansfield ; Brian Egaas ; Kannan Ramanathan, “Low-Cd CIGS Solar Cells Made With a Hybrid CdS/Zn(O,S) Buffer Layer”, IEEE Journal Photovoltaics, October 2016, pp:1-5. 157
  10. A. Giuri, S. Masi, S. Colella, A. Listorti, A. Rizzo, G. Gigli, A. Liscio, E. Treossi, V. Palermo, S. Rella, C. Malitesta, C. E. Corcione, “UV reduced graphene oxide PEDOT: PSS nanocomposite for perovskite solar cells”, IEEE Transactions on Nanotechnology, vol. 15 (5), pp: 725–30.
  11. U. Mehmood, K. Harrabi, I. A. Hussein, and S. Ahmed, “Enhanced photovoltaic performance of dye-sensitized solar cells using TiO<sub>2</sub> – graphene microplatelets hybrid photoanode”, IEEE J. Photovoltaics, vol. 6, Issue 1, 2016, pp: 196–201.
  12. U. Mehmood, S. U. Rahman, K. Harrabi, and I. A. Hussein, “Recent advances in dye sensitized solar cells”, Adv. Mater. Sci. Eng., vol. 2014, Special Issue, 2014, pp: 12.
  13. U. Mehmood et al., “Hybrid TiO<sub>2</sub> – multiwall carbon nanotube (MWCNTs) photoanodes for efficient dye sensitized solar cells (DSSCs)”, Sol. Energy Mater. Sol. Cells, vol. 140, 2015, pp: 174–179.
  14. U. Mehmood, S. Ahmed, I. A. Hussein, and K. Harrabi, “Co-sensitization of TiO<sub>2</sub>-MWCNTs hybrid anode for efficient dye-sensitized solar cells”, Electrochim. Acta, vol. 173, 2015, pp: 607–612.
  15. U. Mehmood, I. A. Hussein, M. Daud, S. Ahmed, and K. Harrabi, “Theoretical study of benzene/thiophene based photosensitizers for dye sensitized solar cells (DSSCs)”, Dyes Pigments, vol. 118, 2015, pp: 152–158.
  16. U. Mehmood, I. A. Hussein, K. Harrabi, and B. V. S. Reddy, “Density functional theory study on dye-sensitized solar cells using oxadiazole based dyes”, J. Photon. Energy, vol. 5, Issue 1, 2015.
  17. U. Mehmood et al., “Photovoltaic improvement and charge recombination reduction by aluminum oxide impregnated MWCNTs/TiO<sub>2</sub> based photoanode for dye-sensitized solar cells”, Electrochim. Acta, vol. 203, 2016, pp: 162–170.
  18. S. Bernardini, S. Johnston, B. West, T. U. Naerland, M. Stuckelberger, B. Lai, M. I.



- Bertoni, “Nano-XRF Analysis of Metal Impurities Distribution at PL Active Grain Boundaries During mc-Silicon Solar Cell Processing”, IEEE Journal of Photovoltaics, Volume: 7, Issue: 1, January 2017, pp: 244 – 249.
19. X. Jin, H. Li, Z. Chen, Q. Zhang, F. Li, W. Sun, D. Li, Q. Li, “Sodium Gadolinium Fluoride Nanophosphor-Based Solar Cells: Toward Subbandgap Light Harvesting and Efficient Charge Transfer”, IEEE Journal of Photovoltaics, Volume: 7 , Issue: 1 , January 2017, pp: 199-205. 158
  20. S. Wasmer, J. Greulich, H. Höffler, N. Wöhrle, M. Demant, F. Fertig, S. Rein, “Impact of material and process variations on the distribution of multicrystalline silicon PERC cell efficiencies”, IEEE Journal of Photovoltaics, vol. 7, issue.1, January 2017, pp:118– 128.